

# Diagenetic facies and reservoir porosity evaluation of deep high-quality clastic reservoirs: A case study of the Paleogene Shahejie Formation, Nanpu Sag, Bohai Bay Basin, China

*Energy Exploration & Exploitation*

2021, Vol. 39(4) 1097–1122

© The Author(s) 2021

DOI: 10.1177/0144598721998504

journals.sagepub.com/home/eea



Jiaqi Yang<sup>1,2,3</sup> , Enze Wang<sup>4</sup>, Youliang Ji<sup>1</sup>,  
Hao Wu<sup>5</sup>, Zhiliang He<sup>3</sup>, Juntao Zhang<sup>3</sup>,  
Yue Zhang<sup>1</sup>, Lingjian Meng<sup>6</sup> and Yue Feng<sup>2</sup> 

## Abstract

Petrological analysis, thin-section observation and laboratory analysis data were selected to systematically study the physical and diagenetic features of the first member of the Paleogene Shahejie Formation ( $E_{s1}$ ) in the No. 3 structural belt of the Nanpu Sag, Bohai Bay Basin. The intensities of different diagenetic processes were determined, the diagenetic evolution sequence was reconstructed, the typical diagenetic facies were identified and the effects of different diageneses on the reservoir were quantitatively analyzed. The results show that the main intergranular fillings include authigenic-quartz, quartz secondary enlargement, clay minerals, carbonate cement and matrix. The pore types include intergranular porosity, dissolution porosity and microfractures. The reservoir has experienced compaction, early cementation, dissolution and

<sup>1</sup>State Key Laboratory of Petroleum Resources and Prospecting, China University of Petroleum (Beijing), Beijing, China

<sup>2</sup>School of Energy Resources, China University of Geosciences, Beijing, China

<sup>3</sup>SINOPEC Exploration and Production Research Institute, Beijing, China

<sup>4</sup>School of Earth and Space Sciences, Peking University, Beijing, China

<sup>5</sup>Key Laboratory of Mineral Resources in Western China (Gansu Province), School of Earth Sciences, Lanzhou University, Lanzhou, China

<sup>6</sup>Research Institute for Exploration and Development, PetroChina Jidong Oilfield Company, Tangshan, Hebei, China

## Corresponding authors:

Youliang Ji, China University of Petroleum Beijing, 18 Fuxue Road, Changping District, Beijing 102249, China.

Email: jiyouliang@cup.edu.cn

Zhiliang He, SINOPEC Exploration and Production Research Institute, Beijing, 100083, China.

Email: hezhiliang@sinopec.com



late cementation, among which compaction is the most important porosity reducer. Compaction was the main diagenetic process involved in porosity reduction, accounting for about 24.4% of the loss of thin-section porosity. The dissolution process clearly improved the porosity, increasing thin-section porosity by 2.7%. Five diagenetic facies were identified on the basis of petrographic analyses, namely, (a) strongly compacted-weakly cemented-weakly dissolved facies; (b) weakly compacted-strongly cemented-weakly dissolved facies; (c) moderately compacted-moderately cemented-weakly dissolved facies; (d) strongly compacted-weakly cemented-moderately dissolved facies; and (e) strongly compacted-weakly cemented-strongly dissolved facies. According to the analysis of diagenesis intensity, the porosity evolution model of various diagenetic facies was reconstructed, and the reservoir quality of various diagenetic facies was quantitatively predicted. The reservoir quality of different diagenetic facies clearly changed with depth. The best reservoir quality was in strongly compacted–weakly cemented–strongly dissolution facies, which have good sorting, contain a large amount of feldspar and soluble debris, and are mainly developed in the main part of the river channel. Our study can provide a reference for the subsequent exploration and development of deep petroleum systems.

### Keywords

Diagenesis, diagenetic facies, porosity evolution, clastic reservoir, Nanpu Sag

## Introduction

The Bohai Bay Basin has always been one of the key basins for oil and gas exploration in China. The Nanpu Sag in Bohai Bay Basin, one of the most-explored oil and gas enrichment areas (Dong et al., 2010; Wang et al., 2011; Zhou et al., 2000), has been explored and developed for many years, and previous studies show that the middle-deep reservoirs in the Nanpu Sag have rich oil and gas potential (Jiang et al., 2018; Pang et al., 2019). Oil and gas exploration has gradually shifted from shallow structural stratigraphic oil–gas deposits (buried at depths less than 3500 m) to lithologic oil and gas deposits in middle-deep layers (buried at depths greater than 3500 m) in recent years (Jin et al., 2018; Lin et al., 2019; Ma et al., 2014; Sun et al., 2013; Zhang et al., 2008). High-quality sandstone reservoirs with a permeability of  $100 \sim 1000 \times 10^{-3} \mu\text{m}^2$ , porosity of more than 15% and relatively coarse grain size have also been found in the deep layer (depth of more than 4000 m) of the No. 3 structural belt, especially in the PG2 oil field, and industrial oil and gas flow has been obtained (Wang et al., 2020a; Wu et al., 2019). Numerous studies have been conducted on the medium-deep reservoirs in the Nanpu Sag, focusing on different aspects including genetic mechanisms, the main controlling factors and the oil and gas resources of high-quality deep reservoirs (Pang et al., 2019; Wang et al., 2019a, 2020a; Wu et al., 2019), however, the study area has strong heterogeneity and complex diageneses (Lai et al., 2018a). Different diageneses lead to great differences in reservoir quality, and there is no systematic study on the diagenetic facies of reservoirs, which restricts the subsequent exploration and development.

Reservoir diagenesis determines porosity evolution (Karim et al., 2010; Wang et al., 2020d; Wu et al., 2019), which can only be systematically studied when the diagenesis is clear, to more accurately guide the subsequent exploration. The final product of diagenesis is the combination of a diagenetic environment and a series of diagenetic events, which is called the diagenetic

facies (Liu et al., 2015; Mou and Brenner, 1982; Wang et al., 2017). Diagenetic facies within the same depth range have theoretically experienced similar diagenetic evolution and the same diagenetic environment, so the reservoir quality within the diagenetic facies is generally similar; therefore, the reservoir porosity in no-well areas can be predicted from the identified diagenetic facies. The method of identifying diagenetic facies by logging interpretation is widely used in areas lacking core data (Ozkan et al., 2011; Selley, 1992).

In this study, the deep Paleogene Es<sub>1</sub> reservoir in the No. 3 structural belt of the Nanpu Sag was selected as an example. The objectives of this investigation were to (a) identify the deep diagenetic facies types by using the logging-interpretation method; (b) reconstruct the diagenetic evolution sequence of the reservoir; (c) quantitatively calculate the influence of diagenesis on reservoir porosity; (d) establish a quantitative evolution model of reservoir quality, through the comprehensive study of reservoir physical properties and diagenesis; and (e) predict the reservoir quality of rocks in the hope of guiding oil and gas exploration and development in the study area more accurately.

## Geological backgrounds

Located in eastern China, the Bohai Bay Basin is the country's second largest petroliferous basin, composed of nearly 50 sub-basins or depressions (Lu et al., 2018). The Nanpu Sag is located in the northeast of the Huanghua depression in the Bohai Bay Basin, adjacent to Yanshan in the north, and the whole depression covers about 1932 km<sup>2</sup> (Dong et al., 2010; Tian et al., 2014; Wang et al., 2011, 2020a, 2020b; Wu et al., 2 019; Zhou et al., 2000). As an important hydrocarbon generating sag in the Bohai Bay Basin, the Nanpu Sag was developed in the basement of the North China platform, which is characterized as a half-graben like depression. In terms of structural unit division, the Nanpu Sag can be divided into two main areas: the continental area including the Beipu, Laoyemiao and Gaoshangpu Liuzan structural belts, and the Nanpu No.1–5 structural belts in the offshore area (Jia et al., 2018; Yuan et al., 2017) (Figure 1).

The sedimentary sequence of the Nanpu Sag is mainly composed of a series of clastic rocks with volcanic rocks, and Cenozoic strata with a thickness of 5000~9000 m is deposited

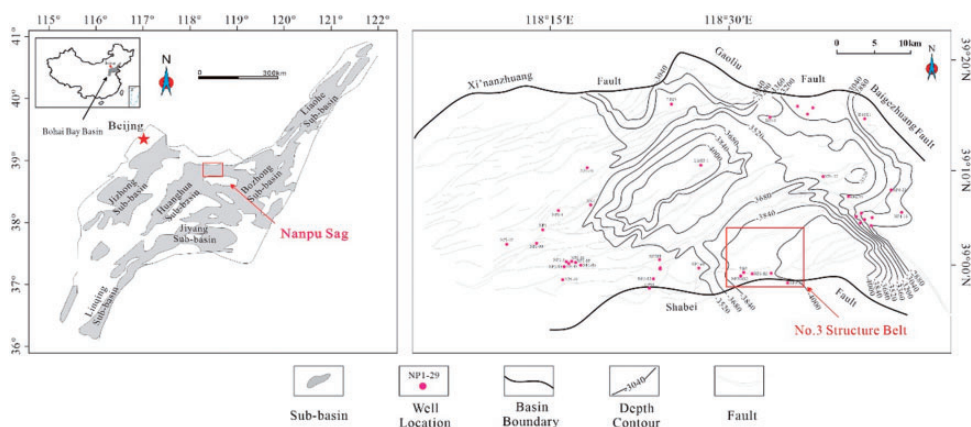


**Figure 1.** Map showing the structural location and distribution of the drilling wells of the No. 3 structural belt in the Nanpu Sag.

(Dong et al., 2010; Guo et al., 2013). The Shahejie (Es), Dongying (Ed), Guantao (Ng) and Minghuazhen (Nm) Formations are deposited from bottom to top. The depositional environment of the Es Formation is braided-river-delta facies, that of the Ed Formation is shore-shallow-lake facies, and the environments of the Ng and Nm Formations are mainly fluvial facies (Guo et al., 2013; Wang et al., 2019b, 2020a, 2020c). The Nanpu Sag experienced the same multi-episodic rifting evolution as the North China platform, forming a number of regional unconformities. The unconformity that formed at the end of the Ed Formation led to an obvious denudation of the Ed Formation stratum. Taking the Gaoliu fault as the boundary, the denudation intensity of the Gaoliu area to the north is relatively high, while the denudation to the south is generally less than 300 m.

Numerous studies have found that three sets of source rocks developed in the Es<sub>3</sub>, Es<sub>1</sub> and Ed<sub>3</sub> Formations in the Nanpu Sag. The reservoirs are mainly distributed in the delta sedimentary facies sand bodies of the Es and Ed Formations and the Neogene fluvial facies sand bodies. The main oil-bearing positions of the No. 3 structural belt are the lower members of the Ed<sub>3</sub> and Es<sub>1</sub> Formations. The volcanic rocks and mudstones widely developed in the Neogene can be used as the regional seal in the study area (Wang et al., 2019b, 2020a, 2020c) (Figure 2).

## Data and methods

A total of 343 core samples from seven exploration wells in the Nanpu Sag were collected, and their porosity and permeability were determined using a core-analysis method (SY/T 5336–2006), routine core-analysis method (SY/T 5336–1996), gas permeability tester (B110) and gas porosity tester (B111) at 25°C and 66% humidity.

The contents of montmorillonite, illite, kaolinite, chlorite, mixed-layer illite and carbonate in 233 samples were determined by X-ray diffraction analysis (XRD). The whole-rock and relative-content analyses of clay minerals were conducted using methods of XRD analysis devised for analyzing clay and common non-clay minerals in sedimentary rocks and an X'Pert PRO diffractometer (B101), at 26°C and 70% humidity.

The particle sizes of 138 samples were analyzed, and the sorting coefficient (So) was determined. A clastic rock particle size analysis method (SY/T 5434–2009), electronic balance and laser particle size analyzer were used for the grading analysis.

The diagenesis was analyzed by casting thin-sections, 92 core samples were injected with blue epoxy and thin-sections under vacuum conditions, and half of the thin-sections were injected with Alisarín Red S to compare and analyze the carbonate minerals. Under the microscope, the pores appear blue, and the carbonate minerals show different colors due to their different compositions. And 15 samples were selected, each sample has at least 8 thin-sections, Point Counting method is employed on the micrographs to estimate the change of thin-section porosity caused by different diageneses. In each thin-section, at least 140 grains were measured following the method of Zhang et al. (2014).

## Results

### *Petrological characteristics*

Based on the analysis of 238 samples from the Es<sub>1</sub> Formation in the No. 3 structural belt, the results show that the quartz content is mostly 21–50% (average, 40.8%), the feldspar

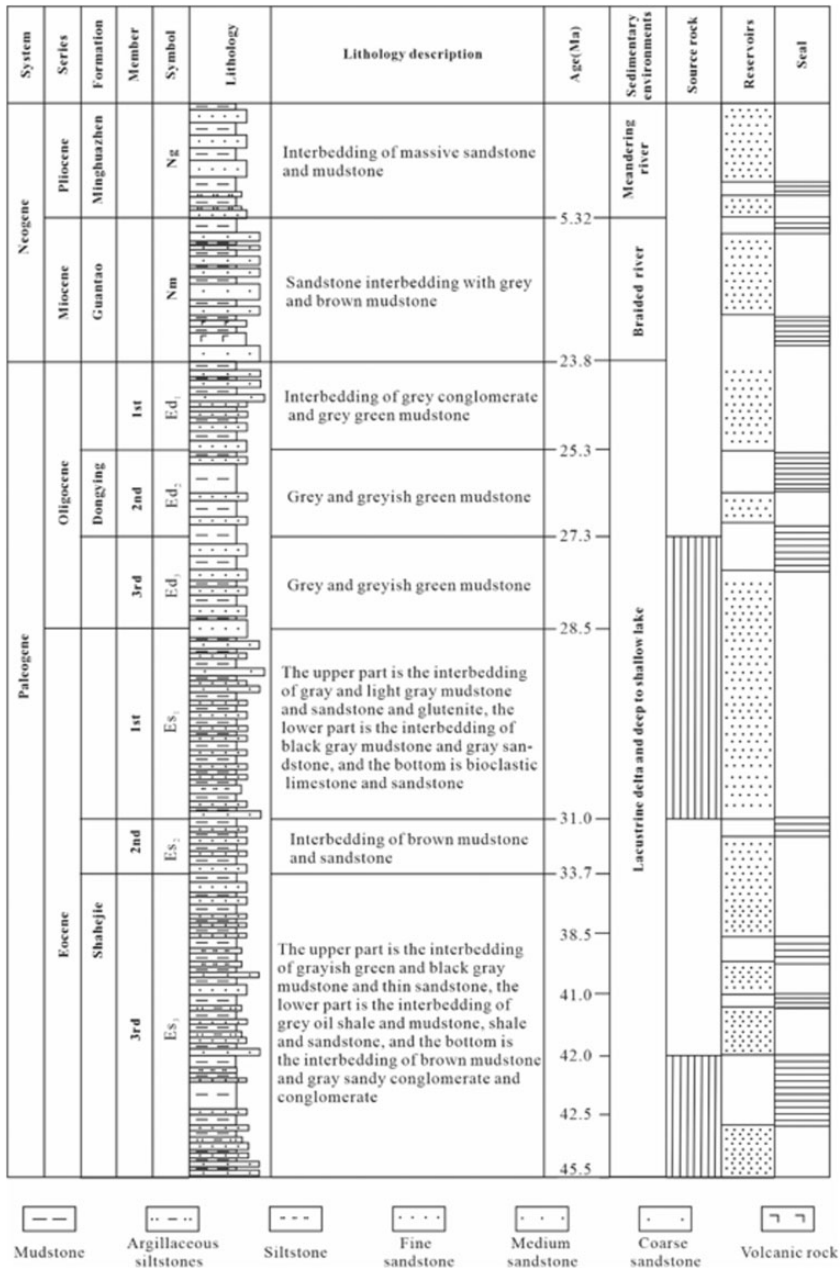


**Figure 2.** Stratigraphic columns of the No. 3 structural belt in the Nanpu Sag (after Dong et al., 2010; Wang et al., 2002).

content is mostly 16–47% (average, 30.8%), and the rock fragment content is mostly 7–54% (average, 20.2%). According to the triangle diagram of the reservoir rock types of the Es<sub>1</sub> Formation, those in the study area are mainly lithic arkose according to the classification form by Folk' (1980) (Figure 3). The sorting coefficients are mainly within the range of

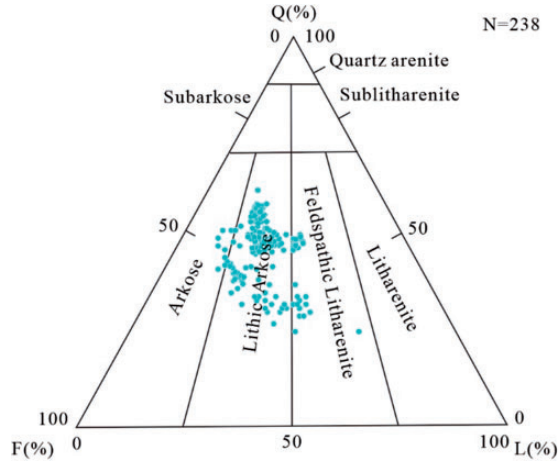


**Figure 3.** Ternary diagram of Es<sub>1</sub> reservoir rock types of the No. 3 structural belt in the Nanpu Sag (after Yang et al. 2020).

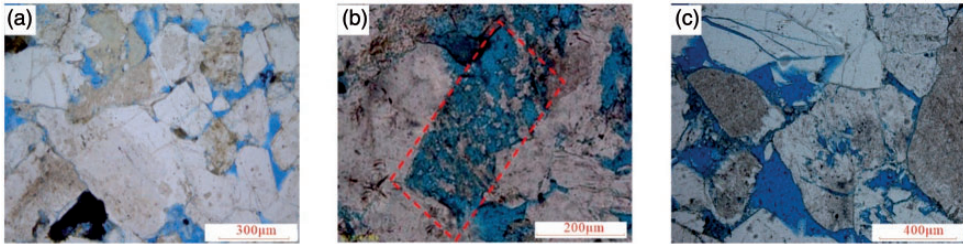


**Figure 4.** The lithology characteristics and pore systems in the Es<sub>1</sub> Formation of the No. 3 structural belt in the Nanpu Sag. (a) Residual intergranular pores, well NP3-82, 4341.51 m, in Diagenetic Facies D, plane—polarized light (PPL); (b) dissolution pore of feldspar, well NP3-82, 4339.5 m, in Diagenetic Facies E, PPL; (c) microfractures of quartz particles broken, well NP306 × 1, 4244.59 m, in Diagenetic Facies D, PPL.

1.05~4.72, with an average of 1.88, and the roundness is sub-angular–sub-circular. The lithology is mainly composed of gravelly sandstone and glutenite with medium structural maturity.

### Pore system

The main types of reservoir pores in the study area are primary and secondary, but the primary pore content is relatively low. According to the casting thin-section identification, the porosity of the primary pores ranges from 0.1% to 7.9%, with an average of 4.8%, while that of secondary dissolution pores ranges from trace to 18.7%, with an average of 8.0%. The primary pores are relatively clear (Figure 4(a)), and the secondary are mainly intra-granular or intergranular pores after the dissolution of feldspar and rock fragments (Figure 4(b)), while particle microfractures can also be observed. Although these types of microfractures have little effect on reservoirs' porosity, they have a relatively large impact

on their permeability. Connected microfractures can greatly increase reservoirs' permeability (Figure 4(c)).

### *Diagenesis and influence on porosity*

The diagenesis of the Es<sub>1</sub> Formation in the No. 3 structural belt, which plays an important role in controlling the reservoir's physical properties, mainly includes medium-strong compaction, various types of cementation and strong dissolution.

**Mechanical compaction.** The depth of the Es<sub>1</sub> member in the No. 3 structural belt is greater than 4000 m, so it has experienced moderate-to-strong compaction. The rock type in the study area is mainly lithic arkose, which contains many plastic particles, such as mica, and its compaction resistance is poorer than that of rigid particles such as quartz. With an increase in reservoir depth, plastic particles become deformed due to compaction, resulting in reduced primary pore space. At the same time, it can be observed under the microscope that some samples with fine grain size contain a large amount of matrix and are strongly compacted, with very low porosity and permeability (Figure 5(a)). The contact mode of particles is generally line contact while it is concave–convex contact for some. In the deep layer, because the overburden pressure is larger than the maximum pressure some particles could bear, some particles fracture along the cleavage crack and form microfractures (Figure 5(b)), which may lead to a great increase in permeability. According to Beard and Weyl's (1973) method, the original porosity of the Es<sub>1</sub> reservoir is 28.4%~35.5%, with an average of 33.1%.

$$OP = 20.91 + 22.9/S_o \quad (1)$$

where OP is the original porosity and S<sub>o</sub> is the sorting coefficient.

The compaction loss porosity (COPL) is calculated with formula (2), and the compaction porosity loss percentage (COPL-P), is calculated with formula (3).

$$COPL = OP - \frac{IGV \times (1 - OP)}{1 - IGV} \quad (2)$$

$$COPL-OP = (COPL/OP) \times 100\% \quad (3)$$

where COPL is the compaction porosity loss, IGV is the intergranular volume and COPL-P is the compaction porosity loss percentage (Houseknecht, 1987; Paxton et al., 2002).

The loss of thin-section porosity caused by compaction is 1.4–33.4% (average, 24.4%), and the compaction rate is 4.5–99.9% (average, 73.2%), therefore, it is the mainly diagenesis that causes the porosity to decrease.

**Cementation.** There are many types of cementation in the Es<sub>1</sub> reservoir of the No. 3 structural belt, including carbonate, siliceous and clay-mineral cementation. The contents of clay minerals and carbonate cement are relatively high, while that of quartz is less than both.

The main types of carbonate cements in the study area are calcite, dolomite and ferro-calcite. There are two phases of carbonate cementation, with contents ranging from 0.6% to

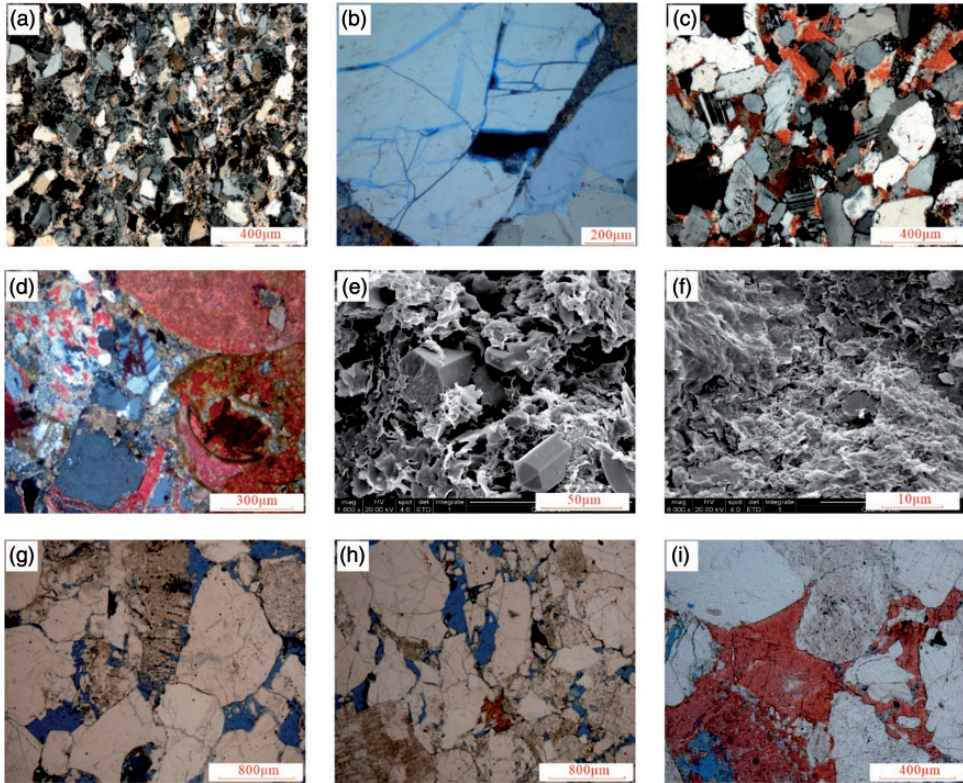


**Figure 5.** Photomicrographs showing the petrography, geochemistry and distribution of diagenetic minerals of the No. 3 structural belt in the Nanpu Sag. (a) The compaction is strong in the greywacke, well PG2, 4249.63 m, in Diagenetic Facies A, cross-polarized light (XPL); (b) quartz particle breakage is accompanied by weak dissolution, well NP3-82, 4925.87 m, in Diagenetic Facies A, XPL; (c) calcite cementation and dolomite replacement occurred on the edge, well NP306x1, 4226.15 m, in Diagenetic Facies B, XPL; (d) carbonate cement filling dissolution pores, well NP3-82, 4925.87 m, in Diagenetic Facies B, XPL; (e) authigenic-quartz and illite cementation, well PG2, 4248.82 m, in Diagenetic Facies A, scanning electron microscope (SEM); (f) mixed-layer illite cementation, well PG2, 4249.66 m, in Diagenetic Facies A, SEM; (g) feldspar dissolution is accompanied by quartz secondary enlargement, well NP306x1, 4234.07 m, in Diagenetic Facies D, PPL; (h) feldspar and rock fragment dissolution, well NP306 × 1, 4223.76 m, in Diagenetic Facies E, PPL; (i) carbonate cement dissolution, well NP306x1, 4240.83 m, in Diagenetic Facies C, PPL.

36.9% (average, 5.9%). The early calcite cement is filled in the primary pores by micrite and sparite or poikilitic. In some sandstones with abundant carbonate cementation, dissolution is weak, carbonate cements occupy almost all the primary pores, and the particles mainly display point contact; at the same time, dolomite replacements can be seen along the edge of the calcite cement (Figure 5(c)). Some samples are characterized by basal cementation, and the rock particles are floating or distributed by point-contact in the early calcite cement. It is considered that cementation should occur before the rock is fully compacted, and that cement can effectively inhibit the later compaction (Morad et al., 2010; Zhong et al., 2007). Some calcite, ferrocalcite and dolomite cement filled feldspar and other secondary dissolution pores, indicating that the formation occurred later than feldspar and debris dissolution (Figure 5(d)).

Mixed-layer illite, illite, chlorite and kaolinite could be identified by SEM and XRD analysis. Regarding the clay mineral cement of the Es<sub>1</sub> Formation reservoir, the content of mixed-layer illite is the highest, followed by that of illite, and the contents of chlorite and kaolinite are lower. The mineral content of authigenic clay ranges from 1.7% to 13.8%, with an average content of 5.5%. The relative content of kaolinite is the lowest, and the absolute content is less than 0.3%. The chlorite content is relatively low due to the relatively low content of volcanic materials and sideromelane minerals in the Es<sub>1</sub> Formation. Chlorite cementation is mainly developed in the distributary-channel sand body of the delta front in the form of a cushion. Mixed-layer illite and illite are abundant and widely distributed. They exist in the grain lining or surface in bridging and filamentous form or directly fill the pores between particles (Dutton and Loucks, 2010) (Figure 5(e) and (f)).

The siliceous cementation in the samples of the Es<sub>1</sub> Formation in the study area is mainly quartz secondary enlargement and authigenic-quartz. The thickness of the quartz enlargement is generally less than 30 μm (Figure 5(g)), characterized by 2–3 stages of enlargement. It appears that the diagenesis is multi-cyclic. It could be observed the authigenic-quartz was filled with intergranular pores under the scanning electron microscope (Figure 5(e)). According to the analysis of thin-sections under the microscope, the volume distribution of quartz cement is 0.5–3.4%, with an average of 1.6%.

The cementation loss porosity (CEPL) is calculated with formula (4), and the cementation porosity loss percentage (CEPL-P) is calculated with formula (5) (Ozkan et al., 2011).

$$\text{CEPL} = (\text{OP} - \text{COPL}) \times \frac{\text{CEM}}{\text{IGV}} \quad (4)$$

$$\text{CEPL-OP} = (\text{CEPL} / \text{OP}) \times 100\% \quad (5)$$

where CEPL is the cementation porosity loss, CEM is the cement content and CEPL-P is the cementation porosity loss percentage.

Cementation leads to a decrease in thin-section porosity from trace to 30.2% (average, 6.7%), and the CEPL-P ranges from trace to 95.3% (average, 8.6%). This plays an important role in controlling the porosity of the study area (Ehrenberg et al., 2008; Higgs et al., 2007; Taylor et al., 2010). However, the overall impact on the reservoir's physical properties is less than that of compaction but still plays an important role in the reservoir's physical properties in the study area.

A plot of total intergranular volume versus total intergranular cement indicates that the loss of depositional porosity due to compaction was greater than that due to cementation (Figure 6). However, in some samples, the effect of cementation appeared to be much greater than that of compaction. The cement contents in these samples were relatively high, mainly carbonate cement, thus filling the pores of the reservoir.

**Dissolution.** There are abundant soluble components in the study area, such as feldspar, some soluble rock fragments, carbonate cement and siliceous cement, which provide the material basis for the dissolution (Hakimi et al., 2012). Many dissolution phenomena could be observed by casting thin-sections.

The dissolution of unstable components such as feldspar and rock fragments are very common (Mansurbeg et al., 2008; Rahman and Mccann, 2012), and secondary pores within

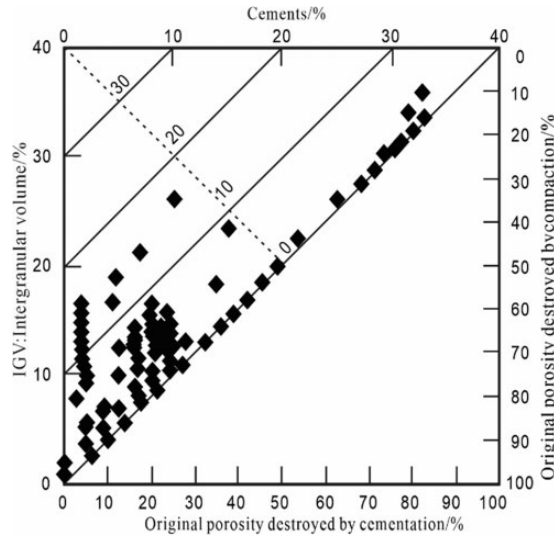


**Figure 6.** Plot of cement volume versus intergranular volume of the No. 3 structural belt in the Nanpu Sag (the plate is from Lundegard, 1992).

and between grains are formed. Acid fluid causes the dissolution of many unstable rock fragments in the reservoir and produces intergranular pores, thus improving the physical properties of the reservoir (Figure 5(h)). In general, potash feldspar is easier to dissolve than acid plagioclase (Yuan et al., 2017). The plagioclase in the reservoir mostly shows partial dissolution, and some feldspar particles are completely dissolved (Nguyen et al., 2018), and they can be identified according to pore shape, residual cleavage and bicrystals (Figure 4(b)).

Due to the early carbonate cementation in the reservoir, this part of cement is easily dissolved under the later action of acidic formation water or organic acids, then, intergranular dissolution pores are developed. At the same time, the pores causing feldspar dissolution are filled with calcite, and this calcite was also found to have been dissolved, indicated that the reservoir had undergone multi-stage dissolution. However, the dissolution of calcite is weaker than that of feldspar and debris.

Compared with that of feldspar and debris, the dissolution of quartz is weak and only occurs at the edge of quartz particles or quartz enlarged edges.

The porosity increase from dissolution (CEPL) is calculated with formula (6), and the dissolution rate (CEPL-P) is calculated with formula (7).

$$CRPI = TP - OP + COPI + CEPI \tag{6}$$

$$CRPI-P = (CRPI/TP) \times 100\% \tag{7}$$

where CRPI is the corrosional porosity increase, TP is the thin-section porosity and CRPI-P is the corrosional porosity increase percentage.

Dissolution leads to an increase in thin-section porosity by trace to 4.7% (average, 1.8%), and the dissolution rate is trace to 91.9% (average, 44.4%). Dissolution is the most important diagenesis for improving the physical properties of the reservoirs in the study area.

**Table 1.** The classification of the extent of influence on the reservoir quality of compaction, carbonate cementation and dissolution.

<i>Intensity</i>	<i>COPL-P/%</i>	<i>CEPL-P/%</i>	<i>CRPI-R/%</i>
Strongly	>70	>70	>50
Moderately	30–70	30–70	30–50
Weakly	<30	<30	<30

Against the overall low porosity and permeability background, the porosity and permeability of some reservoirs are obviously better than those of other reservoirs due to dissolution.

### *Diagenetic facies*

A diagenetic facies is the synthesis of a diagenetic environment, diagenetic products and the material manifestation of a diagenetic environment (Liu et al., 2015; Mou and Brenner, 1982; Wang et al., 2014, 2017). According to the analysis of diagenesis intensity, casting-thin-section and SEM data, the deep reservoirs in the study area are divided into five typical diagenetic facies: (1) strongly compacted–weakly cemented–weakly dissolved facies (Diagenetic Facies A); (2) weakly compacted–strongly cemented–weakly dissolved facies (Diagenetic Facies B); (3) moderately compacted–moderately cemented–weakly dissolved facies (Diagenetic Facies C); (4) strongly compacted–weakly cemented–moderately dissolved facies (Diagenetic Facies D); (5) strongly compacted–weakly cemented–strongly dissolved facies (Diagenetic Facies E) (Table 1).

1. Diagenetic Facies A mainly developed compaction, while cementation and dissolution could not be observed in the thin-sections (Figure 5(a) and 5(b)). Due to the relatively high matrix content, the compaction resistance of the reservoir is relatively poor, and the porosity and permeability are generally low (Henares et al., 2016; Houseknecht and Hathon, 1987; Loucks et al., 1984; Trendell et al., 2012). The reservoir in this type of diagenetic facies is generally fine sandstone and fine siltstone, with a relatively fine grain size and small amount of gravel. The grain contacts are dominated by planar contact, and the particles are weakly or not oriented, a relatively poor diagenetic facies type in the study area.
2. Diagenetic Facies B experienced strong carbonate cementation, and the cement was not dissolved. This type of diagenetic facies is dominated by cementation, the compaction is not strong, and some of the samples contained a small amount of the matrix. Microscopic observations confirmed that many calcites, dolomite and other cements could be observed, and these cements fill spaces between the particles; part of the calcite cement contacts the particles, making dolomite replacement easily (Figure 5(c)). The reservoir in this diagenetic facies is the worst in the study area in terms of its physical properties.
3. Diagenetic Facies C is mainly affected by compaction, and cementation is also an important factor leading to much porosity loss. Weak dissolution improves the physical properties of the reservoir to a certain extent (Figure 5(i)). Microscopic observations confirmed that the reservoir has experienced strong cementation in this diagenetic facies. A great deal of cement fills the pores, consisting mainly of carbonate cements (such as calcite and dolomite), siliceous cements (such as authigenic-quartz and quartz secondary enlargement) and some clay cements (such as illite and mixed-layer illite).

Feldspar and some soluble rock fragments are the main target of dissolution under the microscope. However, most of the dissolution pores are filled with cement.

4. Because Diagenetic Facies D contains many rigid particles, the grain size of the reservoir is relatively coarse and medium coarse sandstone predominates; at the same time, there is abnormally high pressure in the deep layer of the study area (Dong et al., 2014), leading to a porosity reduction of the reservoir in this diagenetic facies caused by compaction during the deposition process is weaker than the other diagenetic facies. Many primary pores can be observed in the deep layer (Figure 4(a)). In comparison, the reservoir in this diagenetic facies is affected by cementation relatively weakly, and only a small amount of late carbonate cements could be observed under the microscope. Compaction and dissolution are the two most important diageneses in Diagenetic Facies D. The main target of dissolution is soluble rock fragments and feldspar. Due to the deep buried depth of the reservoir (greater than 4000 m), some rigid particles (such as quartz) are fractured under the influence of compaction. The microfractures also provide the conditions for dissolution. It could be observed that the main area of dissolution development was around the microfractures (Carvalho and De Ros, 2015). After the acid formation water or organic acids enter the reservoir, some soluble substances will be dissolved and produce a certain amount of secondary pores, which can effectively improve the physical properties of the reservoir.
5. Dissolution greatly influences Diagenetic Facies E. Many mineral particles are dissolved by dissolution, resulting in secondary dissolution pores, and the reservoir's physical properties are greatly improved (Figure 4(b)). The reservoir in this diagenetic facies is generally sorted, and the rock fragment content is generally high. A small amount carbonate cement and authigenic-quartz could also be observed under the microscope. The main target of dissolution is rock debris, therefore this type of reservoir in Diagenetic Facies E has the best physical properties in the study area.

Because of the limited core data, only part of the area and depth can be identified by thin-section observation, so diagenetic facies are often identified by logging (Cui et al., 2017; Lai et al., 2018a, 2018b, 2019; Wang et al., 2017). The logging data for the study area are rich and continuous, so logging interpretation was combined with thin-section data to interpret and analyze the diagenetic facies of the deep clastic reservoir. The logging response of Diagenetic Facies A was characterized by a high acoustic-travel-time logging value (AC) and density-logging value (DEN). The logging interpretation of Diagenetic Facies B is low AC and high DEN, the response characteristics of Diagenetic Facies C are high AC and moderate DEN, the characteristics of Diagenetic Facies D are low AC and moderate DEN, and the logging characteristics of Diagenetic Facies E are high AC and low DEN (Figure 7).

According to the well-log expression of the diagenetic facies, those of deep reservoirs in the study area were identified. Diagenetic Facies A is mainly developed in thin-layer sandstone and at the edge of river channels, Diagenetic Facies B is concentrated at the sand and mud contact boundaries of thick-layer sandstone, Diagenetic Facies C is relatively extensive, and Diagenetic Facies D is mainly developed in underwater distributary channels. The main channels of underwater-distributary-channel microfacies are the most concentrated areas of Diagenetic Facies E (Figures 8 and 9), the best diagenetic facies type in the study area.

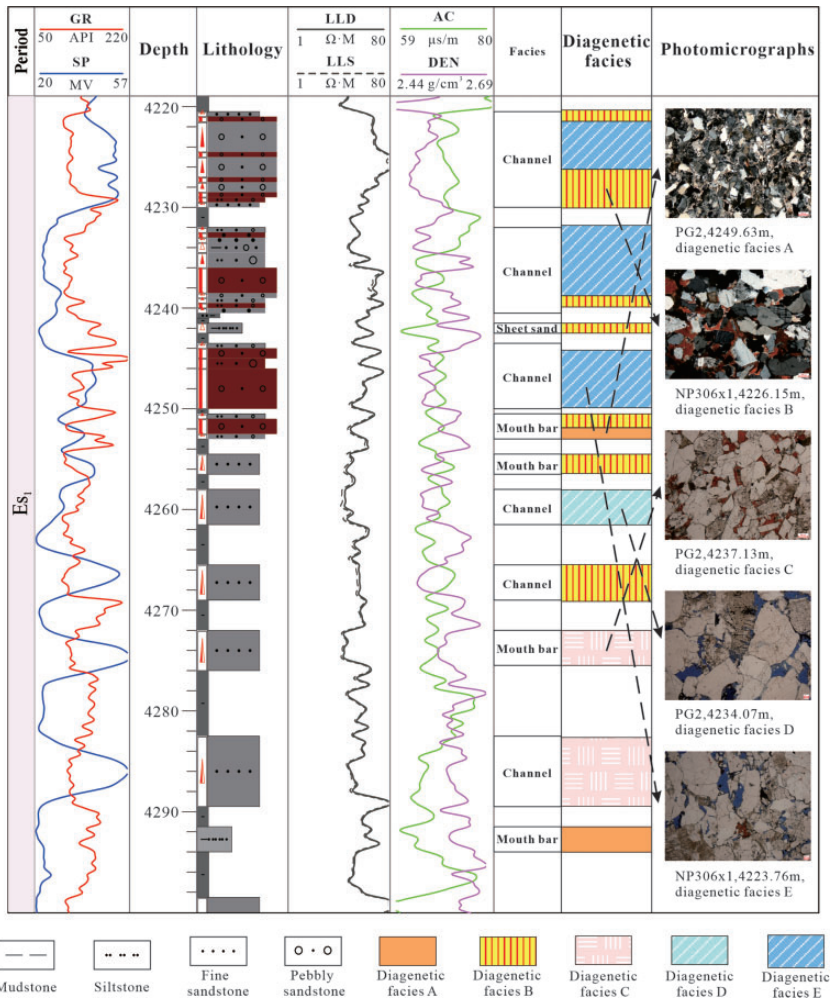


Figure 7. Well log expression and thin-sections of various diagenetic facies.

### Reservoir quality within various diagenetic facies

The analysis of a number of testing data indicated that the porosity of the reservoirs in the Es<sub>1</sub> Formation is 1.5%~15.1% (average, 10.1%) and the permeability is 0.07 ~ 275 × 10<sup>-3</sup> μm<sup>2</sup> (average, 29.9 × 10<sup>-3</sup> μm<sup>2</sup>) (Figure 10).

The porosity of Diagenetic Facies A ranges from 1.5% to 12.4% (average, 7.5%), while the permeability is 0.1~80.1 × 10<sup>-3</sup> μm<sup>2</sup> (average, 1.8 × 10<sup>-3</sup> μm<sup>2</sup>). The carbonate content is generally low, but there is generally much matrix. The matrix contents of some sandstone are more than 30% (Figure 5(a)), and the sorting coefficient is 1.6 ~ 3.3 (average, 2.3). The rock fragment content is relatively high, mainly comprising acidic extrusive-rock debris and

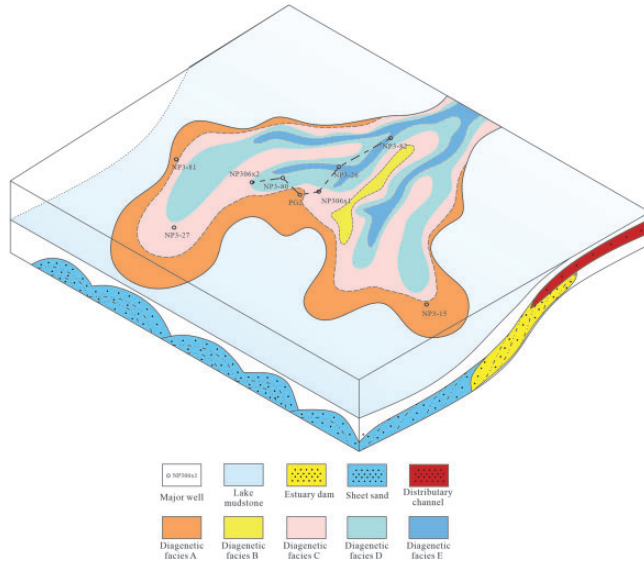


Figure 8. Plan showing the distribution of various diagenetic facies.

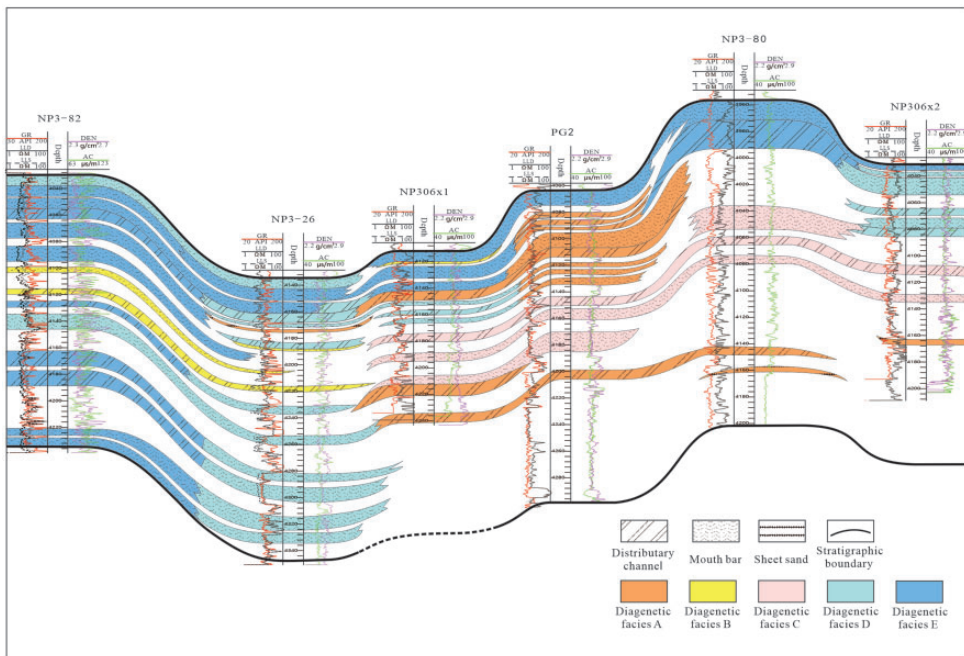
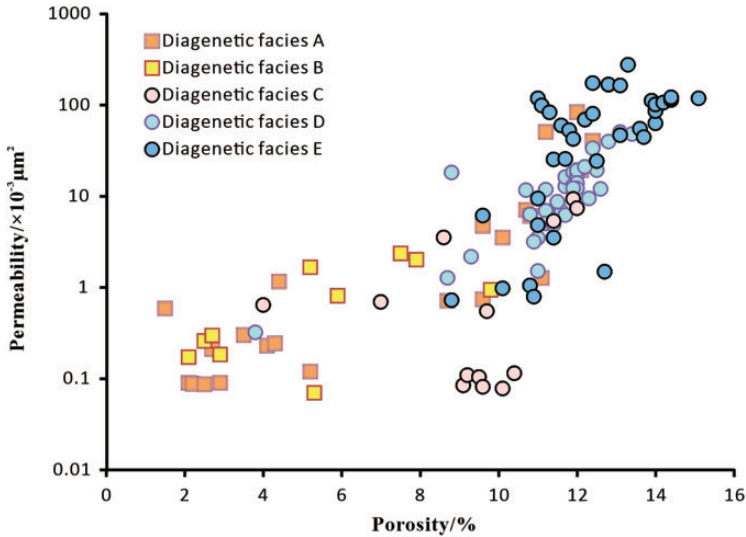


Figure 9. Profile showing the distribution of various diagenetic facies (the survey line is shown in Figure 8) after (Wu, 2018).



**Figure 10.** Cross plot showing the reservoir quality relations of various diagenetic facies.

sedimentary-rock debris, which are relatively soft with weak compaction resistance. During reservoir burial, samples in this diagenetic facies are easily compacted, resulting in the porosity generally being less than 12%. In some relatively pure sandstones, the rigid particles such as quartz and feldspar are crushed by overburden pressure due to strong compaction. Many microfractures are produced, and weak dissolution can later occur along the microfractures under the influence of acidic formation water or organic acids (Figure 5(b)), which have a relatively small impact on porosity but can greatly improve permeability and produce some reservoirs with low porosity and high permeability.

Diagenetic Facies B is affected by strong cementation. As almost no dissolution occurs, the reservoir in this diagenetic facies is the worst in the study area in terms of quality, with almost no porosity and very low permeability. The porosity is 2.1%~9.8% (average, 4.51%), while the permeability is  $0.1 \sim 2.4 \times 10^{-3} \mu\text{m}^2$  (average,  $0.7 \times 10^{-3} \mu\text{m}^2$ ), and the carbonate content is high at 1.2%~30.4%. The sorting coefficient is 1.4~2.5 (average, 1.9). The contact mode between particles is generally point contact (Figure 5(c)), indicating that the cementation is generally developed earlier.

The reservoir physical properties in Diagenetic Facies C are widely distributed, with porosity ranging from 4.0% to 15.6% (average, 9.8%), permeability ranging from approximately 0.1 to  $105 \times 10^{-3} \mu\text{m}^2$  (average,  $9.5 \times 10^{-3} \mu\text{m}^2$ ), carbonate content ranging from 0.4% to 16.3% (average, 3.3%) and the sorting coefficient ranging from 1.5 to 2.2 (average, 1.8). Although the physical properties of the reservoirs in this diagenetic facies are widely distributed, the reservoirs with lower physical properties predominate. The formation of a small number of high porosity and permeability reservoirs is due to the early weak cementation, which can inhibit compaction to a certain extent, but the cement content is lower than that of Diagenetic Facies B, so the lower part of the primary pores can still be preserved in the deep layer, and weak dissolution can simultaneously dissolve some of the early formed carbonate cements (Figure 5(i)), thus improving the reservoir's physical properties.

Diagenetic Facies D has relatively good physical properties, with porosity ranging from 8.1% to 13.4% (average, 11.4%), permeability of  $0.3 \sim 50.4 \times 10^{-3} \mu\text{m}^2$  (average,  $13.8 \times 10^{-3} \mu\text{m}^2$ ) and sorting coefficient of  $1.4 \sim 2.8$  (average, 1.6). In this type of diagenetic facies, the pores are mainly residual-intergranular and partial-dissolution pores. The rigid particles (such as quartz and feldspar) in the sandstone are relatively abundant, and the contents of clay minerals and acid extrusive rock fragments are relatively low in this type of diagenetic facies sandstone; as a result, its compaction resistance is the strongest in the study area. At the same time, due to the existence of abnormal pressure (Dong et al., 2014), the effect of compaction on samples is weaker than that in Diagenetic Facies A during burial, so many residual-intergranular pores can still be preserved in the deep layer, and they can also serve as channels for acidic formation water and organic acids to enter the sandstone; dissolution then occurs, resulting in partial-dissolution pores. The cementation is relatively weak in this diagenetic facies, but there are still some carbonate cements after dissolution, which fill the pores.

The reservoir in Diagenetic Facies E exhibits the best sandstone in the study area, with porosity ranging from 8.8% to 15.1% (average, 12.4%), permeability ranging from 0.7 to  $275 \times 10^{-3} \mu\text{m}^2$  (average,  $73.9 \times 10^{-3} \mu\text{m}^2$ ) and sorting coefficient ranging from 1.5 to 2.5 (average, 1.7). Dissolution greatly influences this type of diagenetic facies. On the basis of a small number of primary pores, a large number of dissolution pores are developed. Throughout the primary pores and microfractures produced by compaction, acidic formation water and organic acids will dissolve many soluble substances (such as feldspar and rock debris) in the sandstone; some particles are completely dissolved, and small amounts of carbonate cement exist in some samples but also experience dissolution.

## Discussions

### *Diagenetic evolution sequence*

Many studies on the diagenetic evolution history of the study area have been carried out (Wu et al., 2019, 2020a; Yang et al., 2020), the vitrinite reflectance ( $R_o$ ) ranges from 0.98% to 1.33%, with an average of 1.14%;  $T_{\text{max}}$  ranges from  $423^\circ\text{C}$  to  $466^\circ\text{C}$ , with an average of  $448^\circ\text{C}$ . The results of the XRD analysis show that the proportion of montmorillonite in mixed-layer illite is 10% ~ 35%, and the average value is 19%. It was determined that the reservoir of  $Es_1$  Formation in the No. 3 structural belt is in the mesodiagenesis stage according to the Chinese standard classification scheme of sandstone diagenesis “the division of diagenetic stages in the clastic rocks” (SY/T5477-2003).

**Eodiagenesis.** In the 40 Ma, the  $Es_1$  started to sediment, due to the strong hydrodynamic deposition environment, the sediments generally processed coarse grain size. In this stage, the sediments stayed in unconsolidated status, therefore, the mechanical compaction had significant influences for reservoirs. The rigid grains were rearranged, and soft plastic grains were deformed, which caused large amount of porosity reduction. Meanwhile, the low mineralization degree caused the alkaline formation water, and this sedimentary environment promoted the deposition of early carbonate cements (Figure 11).

**Mesodiagenesis.** At 28 Ma, the  $Es_1$  entered mesodiagenesis stage A1, in this period, the dissolution of feldspar, some soluble rock fragments and cements played a more important role

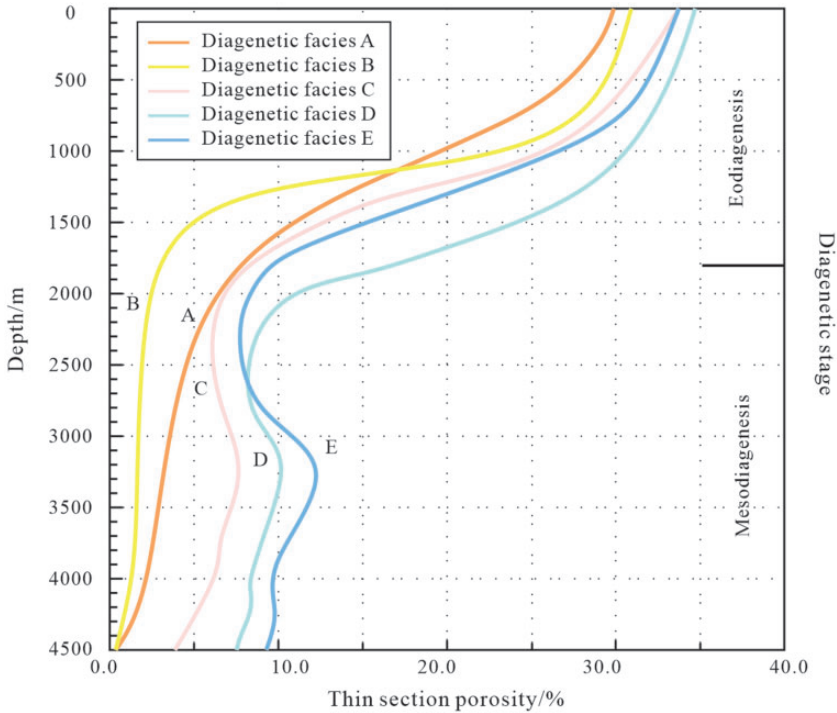


**Figure 11.** Diagenetic evolution sequence of the Es1 Formation of the No.3 structural belt in the Nanpu Sag.

compare with mechanical compaction and cementation (Yang, et al., 2020). Because of high geothermal temperature (90 to 120 °C), source rocks reached hydrocarbon generation threshold, accompanied with this process, large amount organic acid were generated and expelled from source rocks, which promoted the dissolution process and formed many different types of dissolution pores, accompanied by some kaolinite, authigenic-quartz and other mineral precipitation. When the burial depth exceeded 3000 m (about 8 Ma), the Es1 reached mesodiagenesis A2 stage, due to clay mineral transformation and hydrocarbon charging (about 3 Ma, Wang et al., 2020b), the acid formation water environment was weakened and further influenced the intensity of dissolution (Figure 11).

**Reservoir porosity prediction models with various diagenetic facies**

The influence of diagenesis on different diagenetic facies in the study area was calculated quantitatively according to the method described in Section 4.3, and the results are shown in Table 2. Diagenetic Facies A is mainly controlled by compaction (Figure 12). The OP (original porosity) of the reservoir was 30% as calculated with formula (1). Due to the relatively high debris content and poor sorting, the reservoir was greatly affected by compaction in the initial stage of sedimentation, which caused its porosity to decrease rapidly. The average porosity reduction by compaction was 99.9% of the thin-section porosity, and the average porosity is 7.5% today, while the thin-section porosity is close to 0%

(Figure 13). The reservoir experienced strong compaction in the eodiagenesis stage, during which the porosity sharply decreased. In the mesodiagenesis stage, due to the maturity of the organic matter, large amounts of organic acids were produced, but the porosity and permeability of the reservoir were very low, entry to the reservoir was difficult. Therefore, although there were many rock fragments in the sandstone, the dissolution was still very weak and few dissolution pores were produced.

The OP of Diagenetic Facies B was 31.9%. The observation of thin-sections revealed that the main driver of porosity reduction is cementation. According to Table 2, porosity reduction by cementation accounts for 93.6% of the thin-section porosity (Figure 13). It can also be observed in the thin-section that the main type of contact between the particles is point contact, which indicates that the cement appears at the early stage of diagenesis when the compaction is not strong. Meanwhile, a large amount of carbonate cement can further inhibit the compaction (Budd, 2002; Morad et al., 2010; Salem et al., 2000), and dolomite replacement occurs at the edge of the contact between calcite cement and particles, indicating that at least two phases of cementation have occurred (Figure 12).

The initial porosity of Diagenetic Facies C was 33.2%. Both compaction and cementation have certain effects on porosity. Compaction reduces porosity by no more than 70% of the total porosity, while cementation reduces it by more than 30% (Figure 13). Under the microscope, strong carbonate cementation could be observed in thin-sections. In the early stage, much carbonate cement exists between the grains, while at the same time, authigenic-quartz can be observed filling the pores. Some siliceous cements also exist in the pores of sandstones in the form of quartz enlargements. The time of authigenic-quartz and quartz overgrowth is considered to be related to the dissolution of feldspar (Morad et al., 2010; Zhong et al., 2007), which produces a large amount of  $\text{SiO}_2$  providing the material basis for siliceous cementation. Feldspar dissolution occurs after the maturation of organic matter, and during the first large scale stage of hydrocarbon charging, large amounts of organic acids enter the reservoir, resulting in the dissolution of some feldspar, soluble rock fragments and carbonate cement. The improvement of porosity by dissolution in this facies are relatively weak, but some secondary dissolution pores could also be observed in thin-sections, and carbonate cement could be observed in these dissolution pores of feldspar or rock fragments, which indicates that there are two stages of carbonate cementation. The early carbonate cementation occurred in the eodiagenesis; at the same time, the early carbonate cement also slightly dissolved (Figure 5(i)), accompanied by quartz overgrowth and authigenic-quartz precipitation. In the mesodiagenesis stage, due to the transformation of clay minerals and change in the diagenetic environment, the late carbonate cement precipitated again and filled the dissolution pores. Finally, part of the calcite cement is dolomitized, especially at the edge of the cement particle contacts, where calcite was easily transformed into dolomite (Figure 12).

The average porosity of Diagenetic Facies D is 11.4%, and the OP is 34.0%. Dissolution and compaction are the two most important diageneses that affect the reservoir physical properties. This type of reservoir in Diagenetic Facies D has the lowest  $S_o$ , therefore, the highest original porosity in the study area. Due to the relatively high content of rigid particles (such as quartz) with the strongest compaction resistance, and the abnormally high pressure in the deep layer of the study area, many primary pores were preserved (Dong et al., 2014). In the eodiagenesis, mechanical compaction is the main diagenesis, but the compaction resistance of the reservoir is relatively strong, so the porosity reduction caused by compaction in the eodiagenesis stage is relatively low. When the buried depth of

**Table 2.** Assessment of the importance of compaction processes and cementation in reducing porosity in the Es<sub>1</sub> Formation sandstones of the No. 3 structural belt in the Nanpu Sag.

Well	Depth/m	OP/%	CEM/%	IGV/%	GOPL/%	COPL-P/%	CEPL/%	CEPL-P/%	CRPI/%	CRPI-P/%	TP/%	Diagenetic facies
PG2	4250.54	33.57	0.04	1.13	32.81	97.74	0.03	0.09	0.19	20.65	0.92	A
PG2	4249.63	33.22	0	0.06	33.18	99.88	0.01	0.02	-	-	0.03	A
NP306X1	4226.15	32.89	31.02	31.17	2.5	7.6	30.24	91.96	-	-	0.8	B
PG2	4255.46	31.48	30.44	30.5	1.41	4.48	30.01	95.33	-	-	0.74	B
NP306X1	4237.13	35.5	15.4	15.36	23.8	67.02	11.7	32.95	-	-	0.03	C
NP306X1	4220.9	28.36	2.02	8.59	21.63	76.27	1.58	5.57	3.64	41.41	8.79	D
NP306X1	4230.12	34.86	1.64	10.84	26.94	77.28	1.2	3.44	4.74	41.36	11.46	D
NP306X1	4234.07	31.74	1.84	10.13	24.05	75.77	1.4	4.41	3.91	38.33	10.2	D
PG2	4254.09	35.01	1.13	7.14	30.01	85.72	0.79	2.26	3.19	43.11	7.4	D
PG2	4256.37	33.48	5.02	6.22	29.07	86.83	3.56	10.63	0.51	37.5	1.36	D
NP306X1	4218.9	35.3	2	2.9	33.37	94.52	1.33	3.77	0.49	44.95	1.09	D
NP306X1	4244.59	34.81	2.1	9.28	28.14	80.84	1.52	4.38	3.43	39.98	8.58	D
NP3-82	4341.51	35.06	5	9.33	28.37	80.93	3.6	10.26	2.72	46.82	5.81	D
NP306X1	4217.91	28.89	2.1	4.91	25.22	87.3	1.57	5.43	6.31	75.03	8.41	E
NP306X1	4223.76	33.22	1.96	4.48	30.09	90.58	1.37	4.12	7.41	80.81	9.17	E

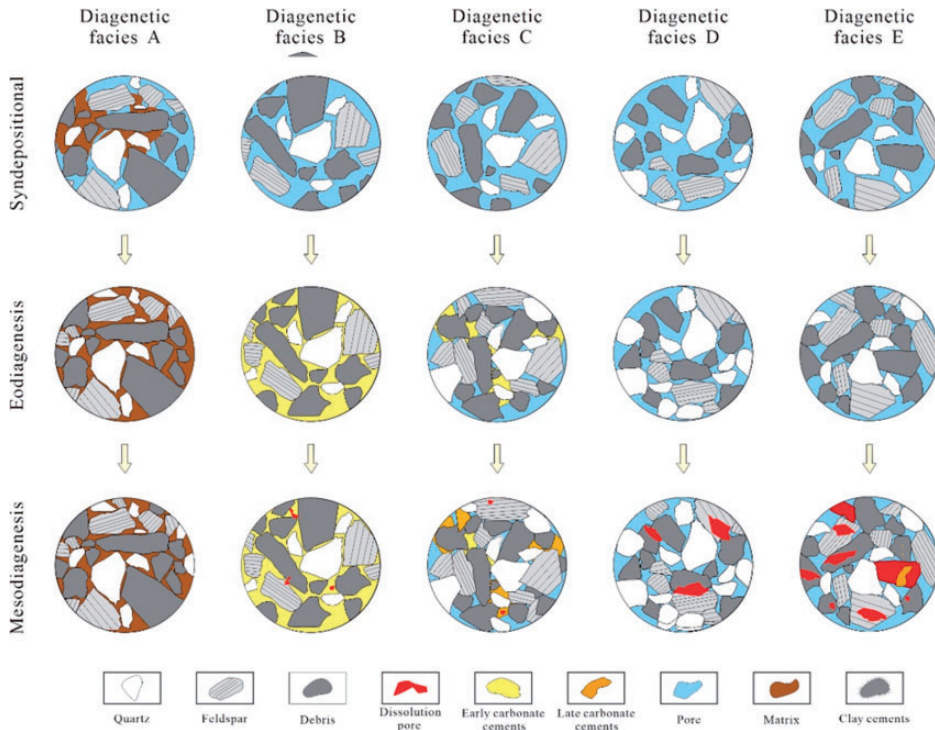


**Figure 12.** Diagenetic evolution pathways for various diagenetic facies within Es1 sandstones.

the reservoir is more than 3, 800 m, because of a large amount of primary pores and the existence of abnormal pressure, the porosity can be resolved in deep reservoir (Jin et al., 2011; Stricker et al., 2016; Wu et al., 2019; Yang et al., 2015). The generation of abnormal pressure in the Nanpu Sag is related to a large amount of mature hydrocarbon expulsion from source rocks (Luo, 2018a, 2018b). Therefore, the generation time of abnormal pressure is after 13 Ma (Meng et al., 2016). At this time, the primary pores of the reservoir in the Diagenetic Facies A, B and C basically no longer exist (Figure 13), therefore the ability of pore preservation by abnormal pressure is relatively weak in others facies. With the occurrence of the first large scale oil and gas migration in the study area, many organic acids entered the reservoir. The existence of a large number of primary pores allowed the formation water to easily move along the connected primary pores, therefore the contact chance of feldspar and soluble cuttings with formation fluid is higher, which leads to more thorough dissolution and more secondary dissolution pores (Figure 12). As a result, the physical properties of the reservoir in Diagenetic Facies D were further improved (Figure 13).

The OP of Diagenetic Facies E was 33.2%, and the CRPI-P is highest in the study area, over 75%. This reservoir has experienced strong compaction and dissolution (Figure 12). Soluble rock fragments are the main target of dissolution. The diagenetic facies mainly developed in the middle of thick-layer sandstone and the main part of a river channel. Under the influence of strong hydrodynamic conditions, the reservoir has relatively good sorting and strong compaction resistance. In the eodiagenesis stage, mechanical compaction is the most important diagenesis, however because these reservoirs are located in the middle

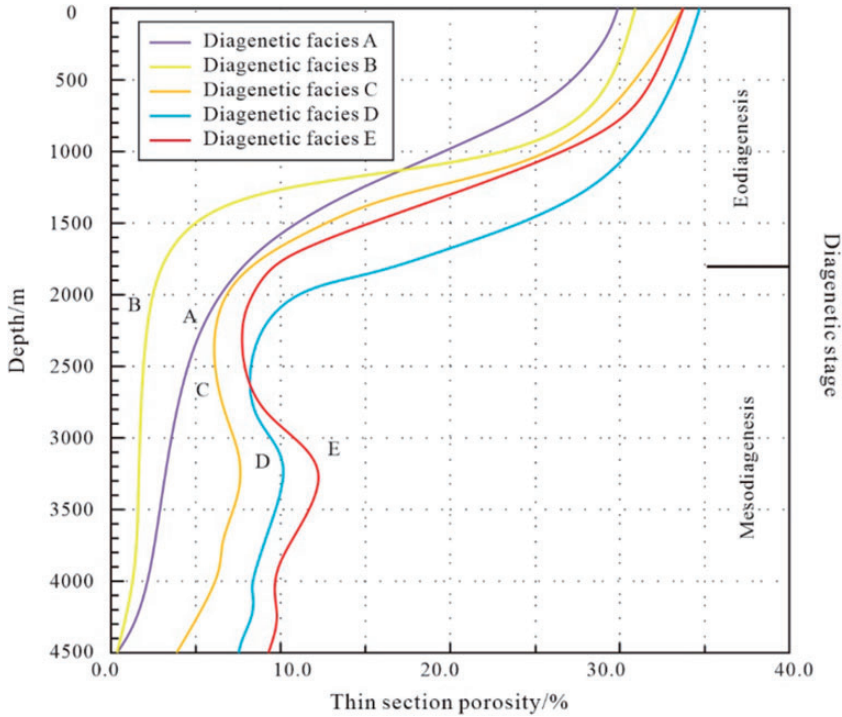


**Figure 13.** Porosity-depth prediction models for various diagenetic facies within Es1 sandstones.

of thick-layer sandstone, the influence of compaction is smaller than that of thin-layer sandstone, resulting a smaller reduction in porosity by early compaction. When source rock enters the mature stage, oil and gas will migrate on a large scale, and the Diagenetic Facies E is located in the main part of the river channel, the dominant channel for oil and gas migration. The existence of abnormal pressure also provides channels for fluids to enter the reservoir by retaining primary pores, thereby promoting the progress of dissolution (Dong et al., 2014; Nguyen et al., 2013). With large amounts of hydrocarbons flowing through the reservoir, organic acids dissolved a large amount of feldspar and many rock fragments and other soluble particles. In the open environment, the dissolved materials continue to move forward with the formation water and hydrocarbons, which ensuring that there is no precipitation in the dissolution pores at the later stage. Consequently, the reservoir in Diagenetic Facies E is the best in the study area (Figure 13) in terms of its porosity and permeability (Bjørlykke and Jahren, 2012).

## Conclusions

1. Dissolution is the most important diagenesis for improving reservoir porosity, while compaction and cementation have an important impact on the reduction in porosity. The main intergranular fillings include authigenic quartz, quartz secondary enlargement, clay minerals, carbonate cement and matrix.

2. In the eodiagenesis stage for the Es<sub>1</sub> Formation of the No. 3 structural belt, the main diageneses are compaction and early carbonate cementation, while those in the mesodiagenesis stage are mainly the dissolution of cement, feldspar and debris and late carbonate cementation.
3. According to microscopic petrographic observations, SEM observation, mineral petrology, and diagenetic mineral and diagenesis analysis, five main diagenetic facies were identified. Diagenetic Facies A refers to strongly compacted–weakly cemented–weakly dissolved facies, Diagenetic Facies B refers to weakly compacted–strongly cemented–weakly dissolved facies, Diagenetic Facies C refers to moderately compacted–moderately cemented–weakly dissolved facies, Diagenetic Facies D refers to strongly compacted–weakly cemented–moderately dissolved facies, and Diagenetic Facies E refers to strongly compacted–weakly cemented–strongly dissolved facies.
4. According to the analysis of diagenesis intensity, the porosity evolution model for various diagenetic facies was reconstructed, and the porosity evolution path and reservoir quality of various diagenetic facies were quantitatively predicted. The best quality reservoir is in a strongly compacted–weakly cemented–strongly dissolved facies with good sorting, containing a large amount of feldspar and soluble debris, mainly developed in the main part of the river channel.

### Acknowledgements

The data of this study were provided by PetroChina Jidong Oilfield Company, and we sincerely appreciate their permission to publish this paper. We are indebted to two anonymous reviewers for their constructive comments, which improved the paper significantly. We also thank the editors of Energy Exploration and Exploitation for their enthusiasm, patience, and tireless efforts.

### Declaration of conflicting interests

The author(s) declared no potential conflicts of interest with respect to the research, authorship, and/or publication of this article.

### Funding

The author(s) disclosed receipt of the following financial support for the research, authorship, and/or publication of this article: The authors would like to thank the China National Natural Science Foundation (No. 42072115); China National Natural Science Foundation (No. 41672098); Major National Science and Technology Project (No. 2016ZX05006-006). Fundamental Research Funds for the Central Universities, (No. lzujbky-2019-1).

### ORCID iDs

Jiaqi Yang  <https://orcid.org/0000-0003-2230-1448>

Yue Feng  <https://orcid.org/0000-0002-0121-3302>

### References

- Beard DC and Weyl PK (1973) Influence of texture on porosity and permeability of unconsolidated sand. *AAPG Bulletin* 57(2): 349–369.
- Bjørlykke K and Jahren J (2012) Open or closed geochemical systems during diagenesis in sedimentary basins: Constraints on mass transfer during diagenesis and the prediction of porosity in sandstone and carbonate reservoirs. *AAPG Bulletin* 96(12): 2193–2214.

- Budd DA (2002) The relative roles of compaction and early cementation in the destruction of permeability in carbonate grainstones: A case study from the paleogene of west-Central Florida, U.S.A. *Journal of Sedimentary Research* 72(1): 116–128.
- Carvalho ADSG and De Ros LF (2015) Diagenesis of aptian sandstones and conglomerates of the campos basin. *Journal of Petroleum Science and Engineering* 125: 189–200.
- Cui YF, Wang GW, Jones SJ, et al. (2017) Prediction of diagenetic facies using well logs – A case study from the upper Triassic Yanchang formation, Ordos basin, China. *Marine and Petroleum Geology* 81: 50–65.
- Dong YX, Xiao L, Zhou HM, et al. (2010) The tertiary evolution of the prolific Nanpu Sag of bohai Bay basin, China: Constraints from volcanic records and tectono-stratigraphic sequences. *Geological Society of America Bulletin* 122(3–4): 609–626.
- Dong Y, Yang S, Chen L, et al. (2014) Braided river Delta deposition and deep reservoir characteristics in bohai Bay basin: A case study of paleogene sha 1 member in the South area of Nanpu Sag. *Petroleum Exploration and Development* 41(4): 429–392.
- Dutton SP and Loucks RG (2010) Reprint of: diagenetic controls on evolution of porosity and permeability in lower tertiary Wilcox sandstones from shallow to ultradeep (200–6700 m) burial, Gulf of Mexico basin, U.S.A. *Marine and Petroleum Geology* 27(8): 1775–1787.
- Ehrenberg SN, Aqrabi AAM and Nadeau PH (2008) An overview of reservoir quality in producing cretaceous strata of the Middle east. *Petroleum Geoscience* 14(4): 307–318.
- Folk RL (1980) *Petrology of Sedimentary Rocks*. Austin, TX, Hemphill Publishing, p. 182.
- Guo YC, Pang XQ, Dong YX, et al. (2013) Hydrocarbon generation and migration in the Nanpu Sag, Bohai Bay basin, Eastern China: Insight from basin and petroleum system modeling. *Journal of Asian Earth Sciences* 77: 140–150.
- Hakimi MH, Shalaby MR and Abdullah WH (2012) Diagenetic characteristics and reservoir quality of the lower cretaceous Biyadh sandstones at Kharir oilfield in the Western Central Masila basin, Yemen. *Journal of Asian Earth Sciences* 51: 109–120.
- Henares S, Caracciolo L, Viseras C, et al. (2016) Diagenetic constraints on heterogeneous reservoir quality assessment: A Triassic outcrop analog of meandering fluvial reservoirs. *AAPG Bulletin* 100(09): 1377–1398.
- Higgs KE, Zwingmann H, Reyes AG, et al. (2007) Diagenesis, porosity evolution, and petroleum emplacement in tight gas reservoirs, Taranaki basin, New Zealand. *Journal of Sedimentary Research* 77(12): 1003–1025.
- Houseknecht DW (1987) Assessing the relative importance of compaction processes and cementation to reduction of porosity in sandstones. *AAPG Bulletin* 71(6): 633–642.
- Houseknecht DW and Hathon LA (1987) Petrographic constraints on models of intergranular pressure solution in quartzose sandstones. *Applied Geochemistry* 2(5–6): 507–521.
- Jiang FJ, Pang XQ, Li LL, et al. (2018) Petroleum resources in the Nanpu Sag, Bohai Bay basin, Eastern China. *AAPG Bulletin* 102(07): 1213–1237.
- Jia HB, Ji HC, Lu CJ, et al. (2018) Sequence stratigraphy and depositional system analysis in paleogene Nanpu Sag: Sequence model and sediment partition. *Geological Journal* 53(4): 1557–1572.
- Jin FN, Zhang KX, Wang Q, et al. (2018) Formation mechanisms of good-quality clastic reservoirs in deep formations in rifted basins: A case study of Raoyang sag in Bohai Bay basin, east China. *Petroleum Exploration and Development* 45(2): 264–256.
- Jin ZK, Su K and Su NN (2011) Origin of Jurassic deep burial high-quality reservoirs in the Central Junggar basin. *Acta Petroli Sinica* v 32: 25–31.
- Karim A, Pe-Piper G and Piper DJW (2010) Controls on diagenesis of lower cretaceous reservoir sandstones in the Western sable Sub-basin, offshore Nova Scotia. *Sedimentary Geology* 224(1–4): 65–83.
- Lai J, Wang GW, Pang XJ, et al. (2018a) Effect of pore structure on reservoir quality and oiliness in paleogene Dongying formation sandstones in Nanpu Sag, Bohai Bay basin, Eastern China. *Energy & Fuels* 32(9): 9220–9232.

- Lai J, Wang GW, Wang S, et al. (2018b) Review of diagenetic facies in tight sandstones: Diagenesis, diagenetic minerals, and prediction via well logs. *Earth-Science Reviews* 185: 234–258.
- Lai J, Fan XC, Pang XJ, et al. (2019) Correlating diagenetic facies with well logs (conventional and image) in sandstones: The eocene–oligocene Suweiyi formation in Dina 2 gasfield, kuqa depression of China. *Journal of Petroleum Science and Engineering* 174: 617–636.
- Lin HM, Liu P, Wang TD, et al. (2019) Diagenetic evolution mechanism of deep glutenite reservoirs based on differences in parent rock types: A case study of lower submember of member 3 of shahejie formation in Chezhen sag, Bohai Bay basin. *Acta Petrolei Sinica* 40(10): 1180–1191.
- Liu HP, Zhao YC, Luo Y, et al. (2015) Diagenetic facies controls on pore structure and rock electrical parameters in tight gas sandstone. *Journal of Geophysics and Engineering* 12(4): 587–600.
- Loucks RG, Dodge MM and Galloway WE (1984) Regional controls on diagenesis and reservoir quality in lower tertiary sandstones along the Texas Gulf Coast. *Clastic Diagenesis* 59: 15–45.
- Lu C, Liu Z, Jia H, et al. (2018) The controls of geomorphology and sediment supply on sequence stratigraphic architecture and sediment partitioning of the lacustrine rift basin in the Es3 of Liuzan area, Nanpu Sag, Bohai Bay basin, China. *Australian Journal of Earth Sciences* 65(2): 275–301.
- Lundegard DP (1992) Sandstone porosity loss; a “big picture” view of the importance of compaction. *Journal of Sedimentary Research* 62(2): 250–260.
- Luo B (2018a) *Characteristics and causes of under-compaction layers of main target formations in Nanpu Sag*. Thesis, University of Petroleum–Beijing, China, 66p.
- Luo R (2018b) *Research on reservoiring mechanism of tight sandstone of Sha 1 Member in the Beach Area of Nanpu Depression, Bohai Bay Basin*. Thesis, University of Petroleum, China, 143p.
- Ma BB, Cao YC, Wang YZ, et al. (2014) Formation mechanism of high-quality reservoir in the middle-deep strata in palaeogene in the North zone of Chezhen depression. *Journal of China University of Mining & Technology* 43(3): 448–457.
- Mansurbeg H, Morad S, Salem A, et al. (2008) Diagenesis and reservoir quality evolution of palaeocene deep-water, marine sandstones, the shetland-faroes basin, British continental shelf. *Marine and Petroleum Geology* 25(6): 514–543.
- Meng LJ, Wu JN, Tang JR, et al. (2016) Evolution and formation mechanism of pressure in the Nanpu Sag. *Geological Science and Technology Information* 35(5): 110–117.
- Morad S, Al-Ramadan K, Ketzer J M, et al. (2010) The impact of diagenesis on the heterogeneity of sandstone reservoirs: A review of the role of depositional facies and sequence stratigraphy. *AAPG Bulletin* 94(8): 1267–1309.
- Mou DC and Brenner RL (1982) Control of reservoir properties of tensleep sandstone by depositional and diagenetic facies; lost soldier field. *Journal of Sedimentary Research* 52: 367–381.
- Nguyen BTT, Jones SJ, Goultly NR, et al. (2013) The role of fluid pressure and diagenetic cements for porosity preservation in Triassic fluvial reservoirs of the Central graben, North sea. *AAPG Bulletin* 97(8): 1273–1302.
- Nguyen DT, Horton RA and Kaess AB (2018) Diagenesis, plagioclase dissolution and preservation of porosity in eocene and oligocene sandstones at the Greeley oil field, Southern San Joaquin basin, California, U.S.A. *Geological Society, London, Special Publications* 435(1): 265–282.
- Ozkan A, Cumella SP, Milliken KL, et al. (2011) Prediction of lithofacies and reservoir quality using well logs, late cretaceous Williams fork formation, Mamm creek field, Piceance basin, Colorado. *AAPG Bulletin* 95(10): 1699–1723.
- Pang B, Dong YX, Chen D, et al. (2019) Main controlling factors and basic model for hydrocarbon enrichment in the sandstone target layer of petroliferous basin: A case study of neogene sandstone reservoirs in Nanpu Sag, Bohai Bay basin. *Acta Petrolei Sinica* 40(5): 519–531.
- Paxton ST, Szabo JO, Ajdukiewicz JM, et al. (2002) Construction of an intergranular volume compaction curve for evaluating and predicting compaction and porosity loss in rigid-grain sandstone reservoirs. *AAPG Bulletin* 86(12): 2047–2067.
- Rahman MJJ and Mccann T (2012) Diagenetic history of the Surma group sandstones (miocene) in the Surma basin, Bangladesh. *Journal of Asian Earth Sciences* 45: 65–78.

- Salem AM, Morad S, Mato LF, et al. (2000) Diagenesis and reservoir-quality evolution of fluvial sandstones during progressive burial and uplift: Evidence from the upper Jurassic boipeba member, Recôncavo basin, northeastern Brazil. *AAPG Bulletin* 84(7): 1015–1040.
- Selley RC (1992) The third age of wireline log analysis: Application to reservoir diagenesis. *Geological Society (London) Special Publications* 65(1): 377–387.
- Stricker S, Jones S, Sathar L, et al. (2016). Exceptional reservoir quality in HPHT reservoir settings: Examples from the Skagerrak Formation of the Heron Cluster, North Sea, UK: *Marine and Petroleum Geology* 77: 198–215.
- Sun LD, Zou CN, Zhu RK, et al. (2013) Formation, distribution and potential of deep hydrocarbon resources in China. *Petroleum Exploration and Development* 40(6): 687–649.
- Taylor TR, Giles MR, Hathon LA, et al. (2010) Sandstone diagenesis and reservoir quality prediction: Models, myths, and reality. *AAPG Bulletin* 94(8): 1093–1132.
- Tian JQ, Hao F, Zhou XH, et al. (2014) Charging of the Penglai 9-1 oil field, Bohai Bay basin, China: Functions of the Delta on accumulating petroleum. *Marine and Petroleum Geology* 57: 603–618.
- Trendell AM, Atchley SC and Nordt LC (2012) Depositional and diagenetic controls on reservoir attributes within a fluvial outcrop analog: Upper Triassic Sonsela member of the Chinle formation, petrified Forest national park, Arizona. *AAPG Bulletin* 96(4): 679–707.
- Wang C, Jin ZG and Liu CZ (2014) Research on diagenetic facies based on diagenetic effect in the low permeability sandstone reservoir – A case from C81 reservoir in Huanjiang region, ordos basin. *Applied Mechanics and Materials* 522–524: 1274–1279.
- Wang EZ, Wang ZJ, Pang XQ, et al. (2019a) Key factors controlling hydrocarbon enrichment in a deep petroleum system in a terrestrial rift basin—A case study of the uppermost member of the upper paleogene shahejie formation, Nanpu Sag, Bohai Bay basin, NE China. *Marine and Petroleum Geology* 107: 572–590.
- Wang EZ, Pang XQ, Zhao XD, et al. (2019b) Characteristics, diagenetic evolution, and controlling factors of the Es1 deep burial high-quality sandstone reservoirs in the PG2 oilfield, Nanpu Sag, Bohai Bay basin, China. *Geological Journal* 55(4): 2403–2419.
- Wang EZ, Liu GY, Pang XQ, et al. (2020a) Diagenetic evolution and formation mechanisms of Middle to deep clastic reservoirs in the Nanpu Sag, Bohai Bay basin, east China. *Petroleum Exploration and Development* 47(2): 343–333.
- Wang EZ, Liu GY, Pang XQ, et al. (2020b) An improved hydrocarbon generation potential method for quantifying hydrocarbon generation and expulsion characteristics with application example of paleogene shahejie formation, Nanpu Sag, Bohai Bay basin. *Marine and Petroleum Geology* 112: 104106.
- Wang EZ, Liu GY, Pang XQ, et al. (2020c) Sedimentology, diagenetic evolution, and sweet spot prediction of tight sandstone reservoirs: A case study of the third member of the upper paleogene shahejie formation, Nanpu Sag, Bohai Bay basin, China. *Journal of Petroleum Science and Engineering* 186: 106718.
- Wang H, Jiang H, Lin ZL, et al. (2011) Relations between synsedimentary tectonic activity and sedimentary framework of dongying formation in Nanpu Sag. *Journal of Earth Sciences and Environment* 33(1): 70–77.
- Wang H, Wang F, Zhou HM, et al. (2002) *Thermal Dynamics and Reservoir Forming Dynamics of the Nanpu Sag in the Bohai Bay Basin (in Chinese)*. Wu Han, China: China University of Geosciences Press, pp. 11–13.
- Wang J, Cao YC, Liu KY, et al. (2017) Identification of sedimentary-diagenetic facies and reservoir porosity and permeability prediction: An example from the eocene beach-bar sandstone in the Dongying depression, China. *Marine and Petroleum Geology* 82: 69–84.
- Wang JJ, Wu SH, Li Q, et al. (2020d) Controls of diagenetic alteration on the reservoir quality of tight sandstone reservoirs in the Triassic Yanchang formation of the ordos basin, China. *Journal of Asian Earth Sciences* 200: 104472.

- Wu H (2018) Genesis and Distribution Prediction of High-Quality Reservoirs of the Paleogene Mid-Deep Horizon in the Southern Nanpu Sag, Bohai Bay Basin, East China. Thesis, University of Petroleum -Beijing, China, p. 161.
- Wu H, Ji YL, Zhou Y, et al. (2019) Origin of the paleogene deep burial high-quality reservoirs in the Southern Nanpu Sag. *Journal of China University of Mining & Technology* 48(3): 553–569.
- Yang T, Cao YC, Wang YZ, et al. (2015) Genesis of high-quality reservoirs of fan Delta front in lower part of the fourth member of shahejie formation in Bonan Subsag. *Earth Science—Journal of China University of Geosciences* v 40: 2067–2080.
- Yang JQ, Ji YL, Wu H, et al. (2020) Diagenesis and porosity evolution of deep reservoirs in the Nanpu Sag: A case study of sha 1 member of the paleogene in no. 3 structural belt. *Acta Sedimentologica Sinica*. <https://doi.org/10.14027/j.issn.1000-0550.2020.061>
- Yuan GH, Cao YC, Zhang YC, et al. (2017) Diagenesis and reservoir quality of sandstones with ancient “deep” incursion of meteoric freshwater: An example in the Nanpu Sag, Bohai Bay basin, east China. *Marine and Petroleum Geology* 82: 444–464.
- Zhang WC, Li H, Li H J, et al. (2008) Genesis and distribution of secondary porosity in the deep horizon of Gaoliu area, Nanpu Sag. *Petroleum Exploration and Development* 35(3): 308–312.
- Zhang XF, Liu B, Wang JQ, et al. (2014) Adobe photoshop quantification (PSQ) rather than point-counting: A rapid and precise method for quantifying rock textural data and porosities. *Computers & Geosciences* 69: 62–71.
- Zhong DK, Zhu XM, Li S J, et al. (2007) Influence of early carbonate cementation on the evolution of sandstones: A case study from Silurian sandstones of Manjiaer depression, Tarim basin. *Acta Sedimentologica Sinica* 25(6): 885–890.
- Zhou HM, Wei ZW, Cao ZH, et al. (2000) Relationship between formation, evolution and hydrocarbon in Nanpu Sag. *Oil & Gas Geology* 21(4): 345–349.